Cotton Fibers Encapsulated with Homo- and Block Copolymers: Synthesis by the Atom Transfer Radical Polymerization Grafting-From Technique and Solid-State NMR Dynamic Investigations

Valter Castelvetro,*[,†,‡] Marco Geppi,[†] Simone Giaiacopi,[†,§] and Giulia Mollica[†]

Dipartimento di Chimica e Chimica Industriale, Università di Pisa, via Risorgimento 35, 56126 Pisa, Italy, PolyLab-CNR, via Risorgimento 35, 56126 Pisa, Italy, and INSTM, via Risorgimento 35, 56126 Pisa, Italy

Received June 22, 2006; Revised Manuscript Received October 5, 2006

Cotton fibers were modified by surface-initiated atom transfer radical polymerization of ethyl acrylate (EA) followed by copolymerization with styrene. Either ethyl 2-bromopropionate as a sacrificial free initiator or Cu(II) as a deactivator was used to optimize the EA grafting yield and to preserve the livingness of the chain ends for the subsequent growth of a poly(styrene) (PSty) block from the poly(ethyl acrylate) (PEA) grafts. The polymer-encapsulated cotton fibers were analyzed by Fourier transform infrared spectroscopy, scanning electron microscopy, differential scanning calorimetry (DSC), thermogravimetric analysis, and solid-state NMR (high-resolution ^{13}C cross-polarization magic angle spinning, ^{1}H spin−lattice relaxation times, and ^{1}H free induction decay analysis NMR). The latter allowed the detection of the dynamic modifications associated with the presence of homo- and block copolymer grafts. In particular, the results of the DSC and NMR investigations suggest a heterogeneous morphology of the *g*-PEA-*b*-PSty grafted skin, which could be described as an inner layer of *g*-PEA sandwiched between the semicrystalline cellulose of the core fiber and the high glass transition temperature PSty of the covalently linked outer layer. Such morphology results in a reduced molecular mobility of the PEA chains.

Introduction

In the last few decades a large number of studies have elucidated the main structural and morphological features of pure cellulose, in relation with its reactivity and with the presence of different crystalline forms and amorphous regions.[1−5] More recently, the main interest in this field has been directed toward the modification of the physical and chemical properties of cellulose-based natural fibers, with the purpose of obtaining new functional materials or preparing high-performance composites based on renewable resources. For this purpose, great efforts have been devoted to the development of new processes and chemistry aiming at modifying the surfaces of cellulose fibers to make them more compatible with synthetic polymers,[6,7] to reduce their hydrophilicity and sensitivity to chemical and biological agents, and to increase their elasticity, and resistance to abrasion and heat.[8]

Through surface-initiated "grafting-from" polymerization the fiber surface can be modified by a wide range of covalently anchored polymer bristles.[9−12] Both conventional[13,14] and, more recently, controlled/living[15,16] polymerization processes have been successfully employed for this purpose. The latter can provide a higher grafting density of nearly monodisperse grafts with well-defined molecular weights and controlled structures (e.g., block copolymers). In case of atom transfer radical polymerization (ATRP)[17−19] initiated from a solid surface, the addition of a comparatively large amount of "sacrificial" free initiator to the polymerization system (monomer, surface-graft initiator, Cu(I) complex catalyst) is required to maintain adequate control of the grafting-from polymerization process.[20] In fact, a larger amount of initiator promotes faster buildup of the concentration of Cu(II) deactivator as a result of some irreversible terminations by radical coupling.[21,22] Direct addition of a small amount of Cu(II) deactivator together with the Cu(I) catalyst has a similar effect on the overall polymerization kinetics, while preventing the formation of a large fraction of ungrafted homopolymer as in the case of the addition of sacrificial free initiator.

Spectroscopic, chromatographic, thermoanalytical, and surface-specific characterization techniques have been employed to investigate the morphology of the modified surface as well as the composition, structure, length, and surface density of the polymer grafts.[17,22] Some of these techniques require that the polymer brush be selectively cleaved and recovered from the solid substrate, a not always trivial task.[23]

However, only a few scattered studies can be found in the literature concerning the solid-state NMR (SSNMR) characterization of polymer brushes anchored on a solid surface, whether inorganic or organic, e.g., the cellulose fiber. In particular, the SSNMR technique was mainly used as a tool for the determination of the grafting yield, the characterization of the morphology of the grafted chains with respect to the cellulose bulk, and the detection of modifications induced in the cellulose domains following the functionalization with the polymer.[24−26]

In the present work natural cotton fibers have been modified with poly(ethyl acrylate) (PEA) and poly(ethyl acrylate-*b*-styrene) grafts (*g*-PEA-*b*-PSty) grown from the surfaces of the fibers after binding a suitable ATRP initiator. Cotton was chosen as the substrate because of its chemical homogeneity (88−96

* Author to whom correspondence should be addressed. Phone: +39 050221 9256. Fax: +39 050221 9320. E-mail: vetro@dcci.unipi.it.
† Università di Pisa.
‡ PolyLab-CNR.
§ INSTM.

10.1021/bm060602w CCC: $37.00
Published on Web 12/24/2006

wt % cellulose in the natural fiber, reaching as much as 99 wt % after the standard scouring and bleaching carried out to remove proteins, pectic-gum-like carbohydrates, ash, and wax) and its relevance in textile, packaging, membrane, and other applications. The possibility of modifying the surface of cellulose with polymer grafts of controlled length and composition, providing hydrophobic, adhesive, and other more sophisticated surface-specific properties, is of obvious interest for many applications.

Both the sacrificial free initiator and the added Cu(II) deactivator approaches have been investigated. The former minimizes irreversible termination and formation of dead grafted chains, therefore being preferred for the cellulose-initiated polymerization of ethyl acrylate (EA). The latter is the technique of choice for the second stage, allowing better control of the block copolymerization of styrene (Sty) upon reinitiation from the activated cotton-*g*-PEA.

Styrene and ethyl acrylate were chosen as the comonomers to allow a straightforward investigation of the graft polymerization process by means of readily available characterization techniques, such as attenuated total reflectance (ATR) Fourier transform infrared (FT-IR) and SSNMR spectroscopies, scanning electron microscopy (SEM), size exclusion chromatography (SEC), and thermal analyses. In particular, the different glass transition temperatures of the two homopolymers of EA and Sty and their mutual immiscibility[27] were expected to facilitate the characterization of each homopolymer domain. High- and low-resolution SSNMR experiments (^{13}C cross-polarization magic angle spinning (CP-MAS), ^{1}H T_1 and ^{1}H on-resonance free induction decay (FID) analysis) were specifically aimed at detecting the structural and dynamic modifications induced in cellulose and PEA domains after the PEA grafting and Sty copolymerization, respectively. The degree of mixing among the immiscible components of the synthesized composite materials could also be investigated.

Experimental Section

Materials. Ethyl acrylate (EA, Aldrich), styrene (Sty, Aldrich), and anisole (Fluka) were distilled from CaH_2 under reduced pressure. Tetrahydrofuran (THF) and pyridine (Py) were distilled from Na/K and KOH, respectively. CuBr (98%, Aldrich) was purified according to the published procedure.[28] Ethyl 2-bromopropionate (EBP, 99%), 2-bromoisobutyrylbromide (BIBB), $CuBr_2$ (99%, stored under nitrogen), and *N*,*N*,*N*′,*N*″,*N*″-pentamethyldiethylenetriamine (PMDETA, >99%) were purchased from Aldrich and used as received. Unbleached cotton fibers were received from Tecnotessile (Prato, Italy).

Techniques. FT-IR spectroscopy was performed on a Perkin-Elmer Spectrum GX instrument equipped with a Spectra Tech horizontal ATR accessory.

SEM was performed on fiber samples sputtered with gold using a JEOL JSM T-300 instrument operating at 12 keV.

The sessile static contact angle with water (θ_S) was determined with a KSV CAM-200 instrument on disks of polymer-grafted cotton prepared by compression molding at room temperature and a 10 ton load using a 13 mm die. The reported values are the averages of at least six measurements with 5 μL bidistilled water droplets.

Molecular weights were determined by SEC from 5 g/L chloroform solutions, using a Perkin-Elmer model 2/2 pump with a Rheodyne 7161 injector, two PLgel Mixed-C columns, a Jasco 830 RI differential refractometer, and a Perkin-Elmer LC-75 spectrophotometric detector, operating at 1 mL/min. A set of polystyrene standards (M_w 2.1, 9, 19, 83, and 233 kDa) was used for calibration.

Differential scanning calorimetry (DSC) and thermogravimetric analysis (TGA) were carried out using a Perkin-Elmer DSC7 equipped with a CCA7 cooling controller operating with liquid nitrogen and a Mettler Toledo 851 TGA/SDTA thermogravimetric and differential thermal analyzer. DSC scans were run at 10 °C/min between −50 and 120 °C; the relevant data were collected from the second heating scan after resetting the thermal history of the material with a first heating and cooling scan. In and Zn standards were used for instrument calibration. TGA scans were performed under a nitrogen purge at 10 °C/min in the temperature range between 25 and 600 °C; an intermediate isothermal step at 130 °C (30 min) was inserted in the temperature scan to ensure complete evaporation of adsorbed water.

^{13}C High-resolution solid-state NMR experiments were performed using a Varian Infinity Plus 400 double-channel spectrometer operating at the ^{13}C Larmor frequency of 100.56 MHz, equipped with two CP-MAS probes for rotors with outer diameters of 7.5 and 3.2 mm. The lengths of both the ^{13}C and the ^{1}H 90° pulses were 4.1 and 2.0 μs for the 7.5 and 3.2 mm probes, respectively. The carbon spectra were acquired using the CP-MAS pulse sequence spinning the sample at 6.0 and 15.0 kHz MAS frequencies and under high-power ^{1}H decoupling conditions, using a relaxation delay of 5−7 s and a contact time of 1 ms.

The ^{1}H spin−lattice relaxation times in the laboratory frame (T_1) were measured by means of a ^{13}C-detected inversion−recovery technique.[29]

The ^{1}H low-resolution SSNMR experiments were carried out on a single-channel Varian XL-100 spectrometer interfaced with a DS-NMR Stelar acquisition system, equipped with a 5 mm probe head, working at the proton Larmor frequency of 25 MHz. In all of the experiments the FIDs were acquired under on-resonance conditions following a solid echo pulse sequence to avoid the dead time effect; the 90° pulse length was 2.7 μs. The echo delay was 12 μs, and the dwell time was 1 μs.

Temperature and MAS rates were always controlled within 0.2 °C and 5 Hz, respectively.

Cotton Fiber Purification. The unbleached cotton fibers were stirred for 60 min at 100 °C in aqueous Na_2CO_3 (2 g/L, at a 1:20 w/v fiber to liquor ratio), rinsed with diluted acetic acid, and then with distilled water to neutrality. The air-dried fibers were further extracted with petroleum ether in a Soxhlet apparatus to remove residual waxes,[30] then vacuum-dried to constant weight (48 h at room temperature), and stored under nitrogen.

Binding of the Initiator to the Surface. The purified fibers (1.5 g) were added under a nitrogen atmosphere to a solution containing 3.0 mL of Py (37 mmol) and 3.0 mL of BIBB (24 mmol) diluted in 100 mL of dry THF.[31] The mixture was stirred at reflux for the given time (15 min, unless otherwise specified), then the fibers were first rinsed, then extracted with ethanol (96%) in a Soxhlet apparatus, conditioned as before by vacuum-drying 48 h at room temperature to a constant weight, and then stored under nitrogen.

Graft Polymerization of Ethyl Acrylate with Sacrificial Free Initiator (CotEA2). CuBr (14.3 mg, 0.1 mmol), anisole (2.0 mL), PMDETA (20.9 μL, 0.1 mmol), and EA (2.16 mL, 19.9 mmol) were introduced into a Schlenk flask under dry nitrogen. The solution turned light green as complex formation occurred. To the reaction vessel degassed with three freeze−pump−thaw cycles were then added, under a dry nitrogen blanket, the surface-modified cotton fibers (0.4124 g) and the free initiator EBP (26 μL, 0.2 mmol). The flask was then placed in a thermostated oil bath and left at 90 °C for 24 h. At the end of the reaction the ungrafted free polymer (PEA), unreacted monomer, and catalyst were removed from the polymer-grafted cotton fibers by Soxhlet extraction with methanol. The polymerization solution and the collected methanol extracts were combined, the solvent was removed with a rotavapor, and the solid residue was taken up with chloroform and eluted through a silica gel column to remove the copper catalyst. The free polymer and the grafted cotton fibers were recovered and vacuum-dried separately.

Graft Polymerization of EA with Cu(II) Deactivator (CotEA3). CuBr (101.6 mg, 0.708 mmol), $CuBr_2$ (5.0 mg, 0.022 mmol), dry anisole (18 mL), and PMDETA (0.154 mL, 0.737 mmol) were introduced under

Table 1. Grafting-From Polymerizations of EA Initiated by Cellulose-BIBB (CotEA*n*) and Block Copolymerizations of Sty from the CotEA Surface (CotEA*n*Sty)

run	EIC[a] (mol/g_{cotton})	free initiator (mol/g_{cotton})	Cu(II)	monomer	polymer yield[b] (%)	grafting yield[c] (%)	weight uptake[d] (%)	expected M_w[e] ($g\ mol^{-1}$)	$\bar{M}_n$[f] ($g\ mol^{-1}$); PDI
CotEA1	0	48×10^{-5}	no	EA	93.5	none	none	10000	12300; 1.14
CotEA2	$\geq 5.9 \times 10^{-5}$	48×10^{-5}	no	EA	95.0	15.5	67	10000	11900; 1.16
CotEA3	n.d.	no	yes	EA	23.3	79.9	21		n.d.
CotEA4	$\geq 6.5 \times 10^{-5}$	no	yes	EA	30.3	72.2	426	301000	66100; 1.35
CotEA5	n.d.	no	yes	EA	n.d.	n.d.	5		n.d.
CotEA2Sty	$\geq 5.6 \times 10^{-6}$	no	yes	Sty	5.2	82.2	138	5700000	34700; 1.56
CotEA5Sty	$\geq 9.0 \times 10^{-7}$	no	yes	Sty	1.7	61.6	11	34000000	32300; 1.45

[a] Effective initiator concentration (lower threshold) calculated from $\bar{M}_n$ of the free polymer fraction (see text); n.d. = not determined due to the total amount of free and graft polymer fractions too low for accurate estimates of $\bar{M}_n$ and weight uptake. [b] Overall monomer conversion by gravimetry. [c] Weight % of grafted polymer (*g*-PEA) against total polymer produced. [d] Weight increase of the cotton fibers due to the grafted polymer. [e] Calculated for a 100% monomer conversion at the given concentration of active initiator; for CotEA1 and CotEA2 the grafted initiator fraction is considered as negligible. [f] Determined by SEC against polystyrene standards.

nitrogen into a Schlenk flask containing a magnetic stirrer. The green solution was stirred for 1 h until Cu(II) was completely dissolved, yielding a darker green solution as a result of complex formation. EA (3.0 mL, 27.7 mmol) and 3.0 mL of the obtained catalyst solution were transferred under a nitrogen blanket into a Schlenk flask containing 0.404 g of initiator-modified cotton fibers. The reaction vessel was deoxygenated with three freeze−pump−thaw cycles, then the excess solution was taken up with a syringe, under a nitrogen blanket, until only 0.971 g of solution wetting the cotton fibers was left. By assuming that the two fractions were homogeneous and uniform, the mixture left on the fibers had the following composition: CuBr (2.75 mg, 0.0191 mmol), $CuBr_2$ (0.141 mg, 0.0006 mmol), PMDETA (4.1 μL, 0.0197 mmol), EA (0.49 mL, 4.5 mmol), and anisole (0.49 mL). The flask was placed in a thermostatic oil bath at 90 °C for 24 h, and the final polymerization product was purified as described previously.

Graft Polymerization of EA with Cu(II) Deactivator (CotEA4 and CotEA5). Following the usual procedure, EA (9 mL, 83.06 mmol) and 0.425 g of surface-modified cotton fibers were added, under a nitrogen blanket, to a Schlenk tube containing CuBr (50.1 mg, 0.349 mmol), $CuBr_2$ (2.4 mg, 0.0107 mmol), anisole (9 mL), and PMDETA (75.2 μL, 0.360 mmol). The polymerization was then started without removing the excess solution, and after 22 h at 90 °C the polymerization products were isolated and purified as usual. Two different surface-modified cotton samples were used, obtained by reacting cotton with BIBB for 15 (CotEA4) and 1 min (CotEA5), respectively.

Block Copolymerization of Styrene onto CotEA-Grafted Cotton (CotEA2Sty and CotEA5Sty). Following the same procedure as CotEA4, the CotEA macroinitiator (0.1427 g of CotEA2 and 0.1481 g of CotEA5 for CotEA2Sty and CotEA5Sty, respectively) were added to a Schlenk flask containing CuBr (63.0 mg, 0.440 mmol), $CuBr_2$ (4.9 mg, 0.022 mmol), styrene (5.0 mL, 43.6 mmol), and PMDETA (96.5 μL, 0.462 mmol). The flask was placed in a thermostatic oil bath at 100 °C for 3 h, then the polymer-grafted fibers were drained, washed several times with acetone to remove the catalyst, and Soxhlet extracted with toluene to remove any free polymer. The polymerization solution was combined with the acetone and toluene extracts, the solvent was removed with a rotavapor, and the solid residue was taken up with chloroform and then poured into a large excess of methanol to precipitate any ungrafted poly(styrene). The reprecipitation procedure was repeated twice to remove the last traces of the catalyst.

Results and Discussion

Unbleached cotton was purified by mild treatment with hot soda lime, followed by extraction with a hydrocarbon solvent to remove any residual noncellulose compounds such as pectic substances, proteins, waxes, pigments, and inorganic salts. These are mainly located in the primary shell of the fiber, particularly on its surface, and can affect fiber reactivity.

Scheme 1. Binding of the Initiator to the Cotton Surface

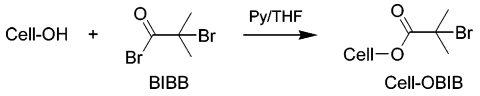

The subsequent reactions were carried out on fibers conditioned to remove most of the absorbed and adsorbed water. While this procedure allowed us to minimize the interference of variable amounts of water and to provide a basis for quantitative measurements by gravimetry, one should take into account that the extensive removal of plasticizing water from the amorphous cellulose domains may result in increased brittleness and partial loss of mechanical strength of the fibers.

Evaluation of the Reactivity of Functionally Modified Cotton under Grafting-From ATRP Conditions. All of the polymerization experiments were carried out using the Cu(I)−PMDETA catalytic complex and variously modified cotton fibers.

In the first experiment (CotEA1 of Table 1), EA was polymerized in the presence of unmodified cotton fibers and EBP as the sacrificial free initiator to ensure the livingness of the process. Under such conditions no grafted polymer could be detected, and the SEC analysis of the polymer recovered from the anisole solution gave a $\bar{M}_n$ value of 12 300 g mol^{-1} with a narrow polydispersity index (PDI), in good agreement with the expected value of 10 000 g mol^{-1} (based on the monomer/initiator molar ratio; 9500 g mol^{-1} upon correction for the actual monomer conversion). This is a clear indication that the presence of the cotton fibers does not affect the controlled ATRP process occurring in solution.

To promote the growth of polymer grafts from the fiber surface a suitable ATRP initiator must be covalently linked to the cotton cellulose. To this purpose the hydroxyl groups of cellulose were reacted with BIBB at refluxing THF (Scheme 1). The resulting ester (cell-OBIB) is known as an efficient ATRP initiating group, its structure being substantially the same as that of EBP.

A large excess of BIBB is required under such relatively mild reaction conditions to achieve a detectable grafting yield, that is, one capable of converting the cotton fiber into an effective initiating surface for the subsequent EA polymerization.

In fact, the first polymerization test carried out using a functional cotton fiber prepared by reaction with a much lower amount of BIBB (1 mol % of the total EA to be used, as in the preparation of polymer grafts of DP = 100 for a theoretical quantitative grafting of BIBB, cell-OBIB initiating efficiency, and monomer conversion) gave no noticeable grafting yield.

A second functionalization reaction was thus performed with

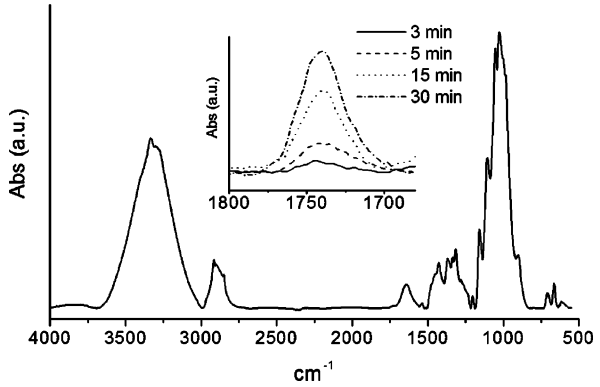

Figure 1. ATR FT-IR spectrum of native cotton fibers, with the characteristic C−O−C stretching bands at 1030 (strongest absorption), 1055, 1108, and 1161 cm^{-1}, the methylene stretching and scissoring at 2900 and 1430 cm^{-1}, respectively, and the broad and strong O−H stretching absorption in the 3600−3100 cm^{-1} range. In the inset (magnification 1.6×) are reported the carbonyl absorptions from the spectra (normalized against the absorption at 1030 cm^{-1}) of the same fibers, taken at different times of the esterification with BIBB (16 mmol/g fibers).

a 100-fold excess of BIBB (16 mmol/g cotton) to allow for the partial hydrolytic degradation of the acyl bromide caused by the residual traces of water, either adsorbed or absorbed on the fiber. Ester formation was confirmed by the presence, in the ATR FT-IR spectrum of the modified fiber, of a weak α-bromo-substituted carbonyl stretching absorption at 1730 cm^{-1} (Figure 1). Further evidence of a brominated group at the fiber surface was obtained by SEM energy dispersive X-ray analysis, although the Br peak was close to the detection threshold. After the first 30 min of reaction, the cotton fibers turned yellow and started breaking apart as a result of extensive esterification, involving not only the fiber surface but also the bulk amorphous regions. Therefore, the modified fiber obtained after 15 min of reaction was employed as the standard substrate for the following experiments of surface-initiated ATRP polymerization.

In particular, CotEA2 was carried out in the presence of cotton fibers grafted with BIBB according to the procedure described previously and adopting the same reaction conditions and feed composition as in CotEA1, that is, Cu(I)−PMDETA as the catalyst and EBP as the sacrificial free initiator. Differently from the case of CotEA1, a comparatively large fraction of grafted polymer (15.5% of the total) was obtained, when considering that the free initiator EBP was in a roughly 10-fold excess with respect to the grafted BIBB.

While under the above conditions the fraction of free (soluble) polymer is necessarily much larger than the grafted one, the presence of such ungrafted polymer is actually helpful, since one can estimate the concentration of active initiator covalently bound to the fiber, or the effective initiator concentration (EIC), by assuming that $\bar{M}_n$ of the free polymer to be equal to that of

$$\mathrm{EIC} \geq \frac{\mathrm{wt}_{\text{grafted polymer}}}{\bar{M}_{n(\text{free polymer})}} \qquad (1)$$

the grafted polymer. Indeed, in our case the actual $\bar{M}_n$ of the grafted poly(ethyl acrylate) (*g*-PEA) could not be measured because the latter could not be effectively cleaved from the cellulose fiber without degradation. All attempts to recover a pure *g*-PEA fraction either by hydrolytic demolition of the cellulose[25,32] or by selective cleavage of the cellulose−polyacrylate ester bond[33,34] were unsuccessful.

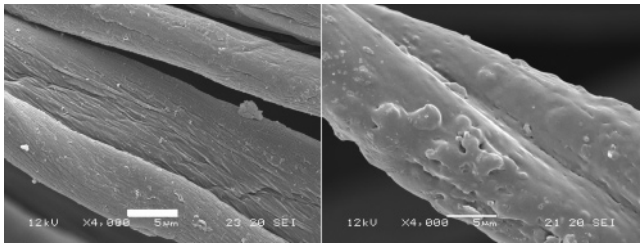

Figure 2. SEM analysis of cotton fibers before (left) and after (right) the grafting of EA in CotEA2. The scale bar is 5 μm in length.

Experimental evidence of a similar molecular weight (M_w) for the free and grafted polymer fractions has been reported by several authors, when the amount of added sacrificial initiator is much larger than that of the surface-grafted initiator, such that the latter can be neglected in the calculation of the expected M_w of the final polymer.[35,36] However, several factors, such as the limited accessibility of the interfacial region for the species involved in the ATRP mechanism of chain growth (monomers and Cu^I and Cu^{II} complexes) or even the presence of a fraction of "dormant" active chain ends, buried within the polymer layer due to chain folding, would still result in higher M_w values and broader molecular weight distributions (MWDs) than in a homogeneous system. Therefore, the EIC should be considered as the lowest threshold for the actual EIC, as indicated in eq 1.

While taking into account the above considerations, a series of experiments carried out using butyl methacrylate (BMA) instead of EA provided further although indirect evidence that the assumption of a close correspondence of M_w for the free (*f*-PEA) and grafted (*g*-PEA) polymer fractions is a fair one. In fact, differently from the case of cellulose-*g*-PEA, the cellulose from cellulose-*g*-poly(butyl methacrylate) (PBMA) could be selectively and quantitatively hydrolyzed, allowing direct determination of M_w's and MWDs of the cleaved PBMA chains by SEC analysis. The relevant experimental details can be found in the Supporting Information.

Surface-Graft Polymerization of EA. As previously mentioned, the synthesis CotEA2 was carried out in the presence of a large excess of sacrificial free initiator. Under these conditions a 67% weight increase of the cotton fibers due to the *g*-PEA fraction corresponded to an EIC of $\geq 5.9 \times 10^{-5}$ mol/g cotton, estimated from the $\bar{M}_n$ of 11 900 g mol^{-1} of the *f*-PEA fraction.

The original macroscopic appearance of the cotton fibers was unchanged after the chemical modification with the exception of a brighter white color related to the increased scattering from the rougher surfaces of the fibers. This can be better seen from the SEM micrographs of the cotton fibers before and after the graft polymerization of EA of CotEA2 shown in Figure 2, where the rough surface of the fibers is clearly associated with a not uniform coating layer of *g*-PEA.

From the ATR FT-IR spectra of Figure 3, one can easily identify the appearance, among the characteristic bands of cellulose, of additional absorption bands due to cotton-*g*-PEA, such as the CH_3 stretching at 2980 cm^{-1}, the C═O stretching at 1727 cm^{-1}, the asymmetric CH_3 bending at 1450 cm^{-1}, and the C—O stretching near 1156 cm^{-1}.

The SEC analysis of the *f*-PEA fractions from both CotEA1 and CotEA2 showed a narrow main peak with a small shoulder at shorter elution times. In Figure 4 are reported the SEC trace and the corresponding deconvolution curves from CotEA2 as a representative example. From the envelope of the SEC trace one obtains a $\bar{M}_n$ value of 11 900 g mol^{-1} and a PDI value of 1.16 (Table 1). The deconvolution, based on the assumption of

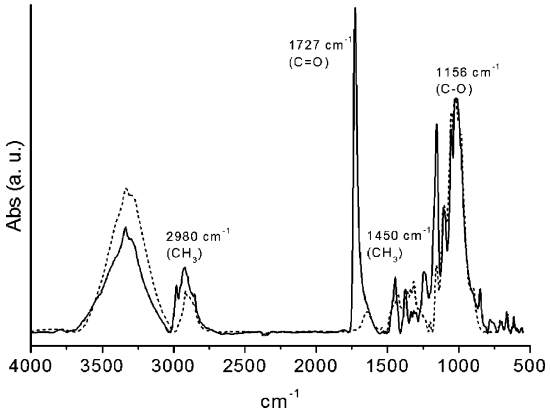

Figure 3. ATR FT-IR spectra of CotEA2 (solid line) and native cotton fibers (dashed line) normalized against the C−O stretching band.

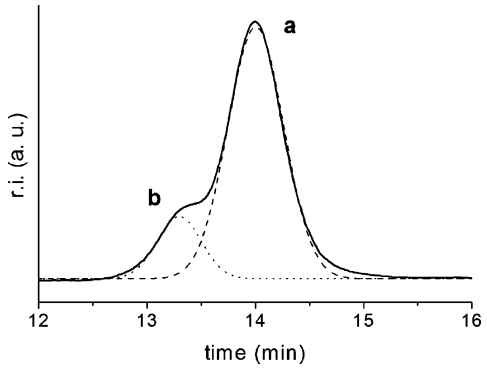

Figure 4. SEC trace for the soluble fraction from CotEA2 (*f*-PEA) and deconvolution curves calculated assuming a bimodal M_w distribution.

a bimodal distribution, gave a low molecular weight fraction (peak a in Figure 4) with a $\bar{M}_n$ value of 11 620 g mol^{-1}, much larger than the high molecular weight fraction (peak b, approximately 15% of the total) with a $\bar{M}_n$ value of 23 110 g mol^{-1}.

Such results are in agreement with common occurrence, even under controlled/living free radical polymerization conditions, of recombination reactions between propagating macroradicals taking place particularly at high monomer conversion.

While the addition of sacrificial free initiator in solution results in a well-controlled polymerization, the method suffers from a low grafting efficiency and the need for painstaking purification procedures to remove the large amount of ungrafted polymer from the polymer-grafted fibers. By replacement of the sacrificial free initiator with an adequate amount of Cu(II) deactivator, fair control of the polymerization can be maintained, while minimizing the formation of ungrafted polymer. The role of the Cu(II) deactivator is that of reducing the concentration of the propagating macroradicals, and thus the rate of the termination reactions, which is characterized by second-order kinetics. Moreover, its presence increases the overall rate of the activation−deactivation catalytic cycle, promoting more uniform growth of all the macromolecular chains.

The following graft polymerizations were thus carried out in the presence of Cu(II) deactivator.

CotEA3 was carried out in the presence of a mere 30 wt % of monomer with respect to the cotton fibers, resulting in the incomplete wetting of the fibers and a not negligible loss of volatile monomer during the freeze−pump−thawing cycles (not considered in the calculation of the monomer conversion). Also in this case the original appearance of the cotton fibers was unchanged after the chemical modification. However, due to the low conversion and the high grafting yield, the amount of collected *f*-PEA was too small for any characterization, and its M_w as well as the EIC could not be measured. Nevertheless the results of CotEA3 gave the first evidence of the effectiveness of the method.

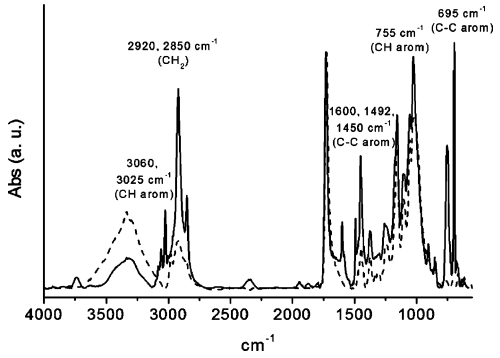

Figure 5. ATR FT-IR spectrum of CotEA2Sty (solid line) and CotEA2 (dashed line) normalized against the C−O stretching band.

To obtain more reliable and complete quantitative data, CotEA4 was carried out in the presence of a large excess of solvent (anisole) and monomer. Under these conditions the overall monomer conversion and grafting yield were approximately the same as those in CotEA3, but the total amount of grafted polymer was much larger. This was probably the result of both a higher average molecular weight of the grafted chains and a higher grafting density, also causing the extensive fracturation observed for the grafted fibers from CotEA4.

In CotEA3 and CotEA4, the formation of a 20−28 wt % ungrafted PEA characterized by a monomodal molecular weight distribution but a comparatively broader PDI can be explained by a too low concentration of Cu(II) deactivator (poorly soluble in anisole/EA), resulting in poorer control of the polymerization process and in the not negligible occurrence of chain transfer and termination reactions. However, the presence of traces of free BIBB initiator as a source of *f*-PEA could not be ruled out.

Surface-Graft Block Copolymerization of Sty from *g*-PEA Macroinitiator. Two different cotton-*g*-PEA samples characterized by a high (CotEA2) and a low (CotEA5) surface density of ATRP-active Br-terminated *g*-PEA chain ends, respectively, were employed for the polymerization of styrene to obtain surface-graft PEA-*b*-PSty copolymers (cotEA*n*Sty, Table 1). Sample CotEA5 was prepared in the usual way from a cotton−OBIB sample obtained by reacting cotton fibers with BIBB for just 1 min (see Experimental Section).

Both CotEA2Sty and CotEA5Sty were carried out in bulk (that is, with a large excess of monomer to homogeneously wet the fibers) and without sacrificial free initiator but in the presence of Cu(II) deactivator, resulting in a comparatively low overall monomer conversion and a still rather high grafting yield. The weight increase of the samples and the ATR FT-IR spectra Figure 5 confirmed the growth of a styrene homo-block (PSty) initiated from the cotton-*g*-PEA brominated "living" chain ends.

Unfortunately, as in the case of cotton-*g*-PEA, all attempts to recover the grafted block copolymers by cleavage from the fibers were unsuccessful. Consequently it was not possible to directly estimate the amount of actively initiating *g*-PEA chain ends because of the lack of SEC data on the *g*-PEA-*b*-PSty copolymer.

As in the case of the EA polymerizations, a fraction of the ungrafted homopolymer (*f*-PSty) was always collected, indicating the occurrence of some uncontrolled chain transfer to monomer and/or homogeneous phase thermal initiation. The

SEC analysis of the *f*-PSty fractions gave monomodal MWDs with PDI values of approximately 1.5, comparatively broader than those in the EA polymerization but still compatible with a controlled interfacial polymerization process. In the case of CotEA2Sty, the EIC, calculated in the usual way, indicates a decreased surface density of growing (living) grafted macromolecular chains, from the initial 5.9×10^{-5} mol/g in CotEA2 to the final 5.6×10^{-6} mol/g in CotEA2Sty. Such reduction is likely to result from a combination of irreversible terminations and kinetically inactive buried chain ends, as discussed previously.

The ATR FT-IR spectra of the polymer-grafted cotton fiber from CotEA2Sty present the same characteristic PEA and cellulose bands as in CotEA2, as highlighted in Figure 5. Additional diagnostic PSty absorptions can be found at 3025 and 3060 (aromatic CH stretching), 2920 and 2850 (backbone CH_2 stretching), 1600, 1492, and 1450 (in plane C−C stretching of the aromatic ring), 755 and 695 (aromatic ring out-of-plane C−H and C−C bending, respectively) cm^{-1}.

As expected, the grafted polymer makes the fiber more hydrophobic. The static contact angles with water of pure cotton could not be measured due to fast absorption. Compression-molded disks prepared with the polymer-grafted cotton gave $\theta = 91°$ (standard deviation $\sigma = 1.3°$) for cotton-*g*-PEA and $\theta = 81°$ ($\sigma = 2.1°$) for cotton-*g*-PEA-*b*-PSty. The lower contact angle measured for cotton-*g*-PEA-*b*-PSty is apparently in contrast with the presence of an outer shell of PSty, since $\theta_{PEA} = 88°$ and $\theta_{PSty} = 90°$ for the pure homopolymer films.[37] However, the apparent higher porosity and surface heterogeneity of the cotton-*g*-PEA plate (with a lower weight fraction of grafted polymer), confirmed by the absorption of the water droplet in less than 1 min after the deposition, did not allow us to draw any straightforward conclusion on the actual composition of the outer surface layer of cotton-*g*-PEA-*b*-PSty.

While in CotEA5Sty the fibers preserve their original flexibility and strength, in CotEA2Sty they become quite brittle and stiff. This is in agreement with the expected more uniform distribution of PEA-*b*-PSty grafts on the fiber surface in the latter, with a phase-separated glassy PSty outer layer. Indeed the combination of the presence of a stiff PSty shell and of the progressive removal, during the successive synthetic and purification operations, of plasticizing water from the cellulose fibers, is likely to lower the flexibility of the fibers to a point that they no longer bear the mechanical stress derived from bending and stretching during their manipulation.

Solid-State NMR. To investigate the presence of both structural and dynamic modifications induced on the cellulose core by the grafting with EA and successive copolymerization with Sty, high- and low-resolution SSNMR experiments were performed on the following samples: pure cotton, CotEA2, CotEA2Sty, and pure PEA (the *f*-PEA fraction from CotEA2). Such measurements consisted of recording high-resolution ^{13}C CP-MAS spectra under high-power proton decoupling conditions, measuring ^1H spin−lattice relaxation times in the laboratory frame (T_1) exploiting the ^{13}C high-resolution, as well as in low-resolution ^1H FID analyses.

^{13}C CP-MAS Spectra. The ^{13}C CP-MAS spectra recorded for the different samples are shown in Figure 6. The spectrum of pure cotton is typical of cellulose (see ref 38 and references therein for a detailed discussion of the assignment of the different resonances and, in particular, of those ascribable to amorphous regions). It consists of the following resonances: 105 (C-1), 89 (crystalline C-4), 84 (amorphous C-4), 75, 72 (C-2, C-3, C-5), and 64 (C-6) ppm.

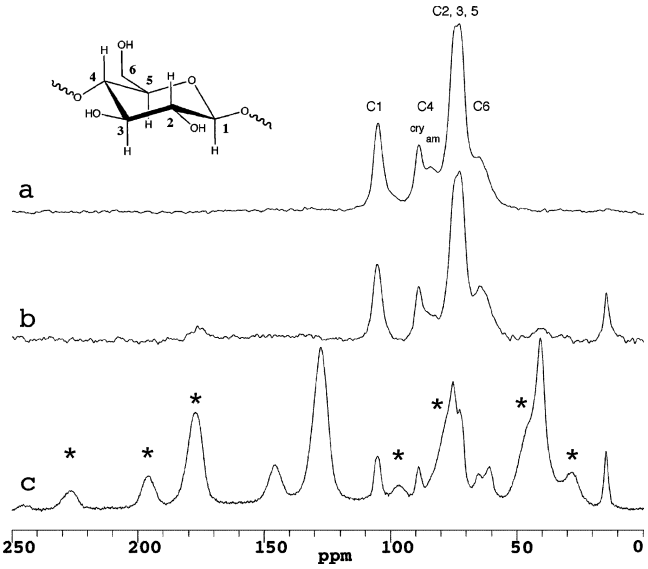

Figure 6. ^{13}C CP MAS spectra of (a) cellulose, (b) CotEA2, and (c) CotEA2Sty. The spinning speed was 6 kHz for both cellulose and CotEA2 and 5 kHz for CotEA2Sty, and the contact time was 1 ms for all the samples. Asterisks denote spinning side bands.

The relative ratio of the peaks at approximately 89 and 84 ppm indicates that in pure cotton cellulose is mostly crystalline. In the CotEA2 spectrum, additional PEA signals can be observed: an intense and clearly distinguishable peak at 15 ppm, due to methyl carbons, two small and large peaks in the 30−50 ppm region, due to main chain CH_2 and CH carbons, and a peak at 175 ppm, due to the ester carbons. The signal arising from CH_2 carbons of the side-chain ethyl group is hidden by the cellulose C-6 resonance. By comparison of CotEA2 and pure cotton spectra no substantial modifications can be observed for cellulose resonances in the 60−110 ppm region, indicating that the grafting process does not remarkably affect the structural properties of the cellulose matrix, in agreement with previous observations.[25] The ^{13}C spectrum of CotEA2Sty shows additional peaks arising from the PSty block attached to the PEA grafts. The main chain CH and CH_2 carbons give rise to a very intense peak at approximately 40 ppm, while the tertiary and quaternary aromatic carbons resonate at approximately 128 and 146 ppm, respectively. Given their large chemical shift anisotropy (CSA), the aromatic PSty signals give rise to several spinning side bands, occurring at multiple frequencies of the spinning frequency (6 kHz in the spectra of Figure 6), partially overlapping some of the cellulose signals. To discriminate between isotropic and spinning side band signals, the spectra of the three samples have also been recorded at a higher MAS spinning frequency (15 kHz, results not shown). Neither the cellulose nor the PEA signals 78 exhibit any detectable change with respect to the corresponding spectrum of CotEA2, thus suggesting the absence of dramatic structural changes caused by the copolymerization with PSty.

^1H FID Analysis. To try to understand the modifications induced on the molecular dynamics of the different components of the systems investigated after each synthetic step (EA grafting and Sty copolymerization) as well as to extract information about both the number and the mobility of dynamically distinguishable domains, a low-resolution ^1H FID analysis has been performed on all the samples. This method has already proven useful when applied to biomacromolecules[39−41] and block copolymers.[42] The FIDs, recorded on-resonance, have been reproduced by means of a nonlinear least-squares fitting procedure, using a linear combination of different analytical functions, chosen among

Table 2. ^{1}H FID Analysis Results at 20 °C for Pure Cotton, PEA (*f*-PEA from CotEA2), CotEA2, and CotEA2Sty samples

component	parameters	cotton	PEA	CotEA2	CotEA2Sty
I exp	wt %	17.2	1.8	10.2	3.4
(mobile regime)	T_2 (s)	280	1390	436	246
II exp	wt %		45.5		
(mobile regime)	T_2 (s)		109		
III exp	wt %		52.7	32.9	5.5
(intermediate regime)	T_2 (s)		31.9	41.7	40.0
Pake	wt %	82.8		56.9	
(rigid regime)	β (s^{-1})	53 400		51 700	
	R_{HH} (Å)	1.82		1.82	
	"effective" T_2 (s)	13.4		13.5	
Gaussian	wt %				91.1
(rigid regime)	T_2 (s)				15.7

Gaussian, exponential, Pake, Weibullian, and Abragamian. After an accurate screening of all the possible combinations, the functions actually employed in our case were the first three, whose expressions are provided as Supporting Information.

The Pake function is characterized by the parameters R_{HH} and β, which, in the original formulation represent the distance between two nearest-neighbor protons and the width of the Gaussian line due to the dipolar interactions between non-nearest-neighbor protons, respectively. In complex polymeric systems, where no isolated couples of protons are present, R_{HH} must be thought of as an average parameter. To have a single parameter indicating the decay rate for the Pake function, an "effective" T_2 can be defined as the time value at which the intensity of the function is reduced by a factor *e* with respect to the time zero.[43]

The parameters characterizing the decay of each function, together with its weight, were optimized by the fitting procedure and give indications about the rate of the dynamic process and the relative percentage of protons belonging to each domain, respectively. T_2 values, or equivalent decay parameters, are approximately 10−20 μs in the "rigid lattice regime" (occurring when the molecular motions have characteristic frequencies lower than the static line width, usually of the order of tens of kilohertz), and it monotonically increases with increasing motional characteristic frequencies above this limit. The complete results of these analyses are shown in Table 2, while the FID analysis of cellulose is reported in Figure 7 as an example. Different sets of functions were necessary for obtaining the best phenomenological reproduction of the FIDs in the different samples (one exponential and one Pake function, three exponentials, two exponentials, and one Pake function, one exponential and one Gaussian function, in the cases of pure cotton, pure PEA, CotEA2, and CotEA2Sty, respectively), thus rendering very difficult a comparison of the dynamic behavior among different samples.

To facilitate such a comparison, three different dynamic regimes have been identified in each sample on the basis of the values of T_2 or "effective" T_2. In particular, a distinction among "rigid", "intermediate", and "mobile" regimes has been performed, corresponding to $T_2 < 20$ μs, 20 μs $< T_2 <$ 100 μs, and $T_2 > 100$ μs, respectively. On one hand, it is clear that this distinction in three regimes oversimplifies the complex dynamic behavior present in the different domains of the samples, but on the other hand, we believe that it can be effective in highlighting the main changes in the molecular dynamics occurring in passing from one sample to another, ascribable to either EA grafting to cellulose or Sty copolymerization. The results obtained grouping the FID fitting functions in this way are reported in Table 3, where they are also compared with the results expected on the basis of the known weight percentages of the different components. Pure cotton shows a high percentage of the rigid phase (82.8%), described by the Pake function, and a small percentage of the mobile component, in good agreement with previous studies;[44] the results for pure PEA, whose FID is reproduced by the sum of three exponential functions, indicate the absence of rigid domains and a substantial equivalence between intermediate (third exponential, 52.7%) and mobile (first and second exponentials, 47.3%) domains. The FID of the CotEA2 sample is well reproduced by a sum of one Pake and two exponential functions: 10%, 33%, and 57% of the protons to be present in mobile, intermediate, and rigid domains, respectively. This result is quite different from that expected on the basis of the FID results of pure cotton and PEA, indicating a remarkable increase of rigid and intermediate domains to the detriment of the mobile component, suggesting that the PEA chains undergo a substantial stiffening when grafted to the cellulose surface. The FID of the CotEA2Sty sample has been reproduced by a sum of one Gaussian and two

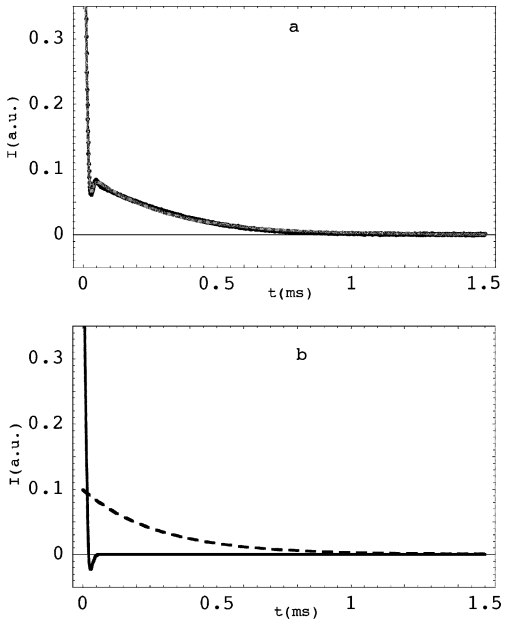

Figure 7. ^{1}H FID analysis of cellulose: (a) experimental and fitted FID (black and gray solid line, respectively); (b) contributions of individual fitting functions exponential (dashed line) and Pake (solid line). The FID was recorded by a solid echo experiment, using an echo delay of 12 μs and a dwell time of 1 μs.

Table 3. Percentage of Protons Belonging to Mobile (T_2 > 100 μs), Intermediate (20 μs < T_2 < 100 μs), and Rigid (T_2 < 20 μs) Regimes (See Text), as Derived from the FID Analysis Results of Table 2[a]

motional regime	pure cotton from FID	pure PEA from FID	CotEA2 from FID	CotEA2 estimated	CotEA2Sty from FID	CotEA2Sty estimated
fast	17%	47%	10%	31%	3%	4%
intermediate	0%	53%	33%	24%	6%	13%
slow	83%	0%	57%	45%	91%	83%

[a] The column "CotEA2 estimated" refers to the percentage of protons calculated from the FID analysis results of pure cotton and pure PEA. The column "CotEA2Sty estimated" refers to the percentage of protons calculated from the FID analysis results of CotEA2, and assuming that all of the PSty protons are in the rigid motional regime. The estimated percentages have been calculated by taking into account the weight percentages of the different components in CotEA2 and CotEA2Sty (Table 1) as well as the weight percentages of protons in the different components (6.2%, 8.0%, and 7.7% in cellulose, PEA, and PSty, respectively.

Table 4. Proton Spin−Lattice Relaxation Times in the Laboratory Frame (T_1), Measured for the Different Components (Cotton, PEA, and PSty) in Each Sample[a]

	component ^{1}H T_1 (s)		
sample	cotton	PEA	PSty
pure cotton	1.83		
pure PEA		1.30	
CotEA2	0.98	0.82	
CotEA2Sty	0.55	0.64	0.75

[a] The reported values are obtained by exploiting the ^{13}C spectral resolution (see Experimental Section) at 20 °C and are the averages of the values measured for the different peaks belonging to each component (maximum error 5%).

exponential functions. The three FID components belong to the three different dynamic regimes, whose weight percentages are now 91%, 6%, and 3%, going from the rigid to the mobile regimes. Also in the hypothesis that all PSty chains are in a rigid environment, the FID analysis for CotEA2Sty indicates a further stiffening caused by the grafting of PSty on CotEA2, resulting in a reduction of the intermediate component from the expected 13% to 6% and in a corresponding increase of the rigid component. Once again, this stiffening should mainly involve PEA chains, since PEA is the only pure component having protons in an intermediate dynamic regime, and indeed they should be more affected by changes in the dynamics, being directly attached to the PSty block.

^{1}H Spin−Lattice Relaxation Times. The dynamic behavior in the megahertz regime and the degree of mixing on a 100 Å spatial scale among the different components have been investigated in the analyzed samples through the measurement of ^{1}H spin−lattice relaxation times in the laboratory frame (T_1) under high-resolution conditions, i.e., via CP with ^{13}C nuclei. In solid samples the energy of the systems is usually redistributed among the different protons via homonuclear dipolar couplings before being exchanged with the surrounding lattice. This process, known as spin diffusion, tends to average the relaxation times of the different protons in a sample to a single value. This average is complete in the case of a sample homogeneous on a scale of approximately 100 Å, while different relaxation times can be measured for protons belonging to different domains with average linear dimensions larger than 100 Å.[45] Given the poor proton spectral resolution, these measurements can be carried out by applying the standard inversion−recovery technique on the proton channel, followed by ^{1}H−^{13}C CP, thus exploiting the high ^{13}C spectral resolution.

The results of the ^{1}H T_1 measurements performed at 20 °C for the different samples are shown in Table 4. In all of the samples, each of the different components (cotton, PEA, and PSty) shows a unique, averaged, ^{1}H T_1 value within the experimental error. As far as the cotton component is concerned, this is in agreement with the intimate mixing between crystalline and amorphous regions of cellulose observed by means of two-dimensional ^{13}C spin−diffusion experiments.[46] However, in both CotEA2 and CotEA2Sty samples, the different components exhibit slightly different T_1 values, indicating that the averaging process carried out by spin diffusion is not complete, i.e., that the different components are not completely mixed on a 100 Å scale. In CotEA2 the PEA component shows the lower relaxation time, therefore representing the relaxation sink for the whole sample. This indicates that motions occurring in PEA are more effective in relaxing protons, i.e., have characteristic frequencies closer to the proton Larmor frequency ω_0 of 400 MHz. This is not surprising, since also in the pure components T_1(PEA) < T_1(cotton). However, it must be noticed that, in absence of modification of the dynamic behavior, the population-weighted relaxation rate (PWRA), defined as[47]

$$\sum_i \frac{w_i}{T_1^{\,i}} \qquad (2)$$

(where i runs over the different components of the sample and w_i represents the protons' weight percentage in the ith component) should not change, being unaffected by spin diffusion. This quantity is in CotEA2 sensibly higher (1.11 s^{-1}) than that in pure PEA (0.77 s^{-1}), despite the presence of slower relaxing cellulose protons, suggesting that the intrinsic relaxation times of PEA strongly decreased in passing from pure PEA to CotEA2. This might be in principle ascribable to a sensible change in PEA dynamics or to the occurrence of additional relaxation mechanisms. Indeed, the motions responsible for relaxation in pure PEA are in a fast motional regime (i.e., $\omega_0\tau$ < 1, τ being the correlation time of the motion), as indicated by the increasing trend of T_1 measured at increasing temperatures above 20 °C (results not shown). The reduction in the intrinsic values of T_1(PEA) on passing from pure PEA to CotEA2 is therefore in agreement with the stiffening of PEA following EA grafting to the cotton fibers, previously deduced from FID analysis results.

The further increase in T_1 PWRA values observed following Sty copolymerization (1.48 s^{-1}) could be in principle ascribable to a further stiffening of PEA chains, again in agreement with FID analysis results. However, in this case, it is possible to observe that the shortest T_1 is now that of cotton protons, instead of PEA ones. This behavior is very difficult to be explained by dynamic behavior only, and it probably has to be ascribed to the presence of residual paramagnetic Cu(II) ions in the cotton domains, which could represent a significant relaxation pathway for protons.

Thermal Characterization. The influence of the grafted PEA chains on the thermal behavior and thermal stability of the modified fibers was investigated by DSC and TGA. The results are summarized in Table 5.

Table 5. Thermal Properties of the Polymer-Grafted Cotton Fibers[a]

sample	T_g (°C)	Δc_p ($Jg^{-1}K^{-1}$)	$T_{d,10}$[b] (°C)	$T_{d,max}$[c] (°C)	R_{600}[d] (wt %)	Δw(pol)[e] (%)	*g*-polymer[f] (wt %)
cotton			338	361	17	0	0
f-PEA	−19	39×10^{-3}	358	403	7	93	n.a.
cotton-*g*-PEA	−10	4×10^{-3}	319	354, 400	10	27	40
cotton-*g*-PEA-*b*-PSty	46	5×10^{-3}	334	341, 431	6	72	75

[a] Data from samples CotEA2 and CotEA2Sty for cotton-*g*-PEA and cotton-*g*-PEA-*b*-PSty, respectively [b] Temperature at 10% weight loss by TGA (N_2, 10 °C/min). [c] Temperature at maximum weight loss rate by TGA. [d] Residue at $T = 600$ °C by TGA. [e] Fractional weight loss due to pyrolytic decomposition of grafted polymer, by TGA. [f] Weight % of grafted polymer in the modified cellulose (from the weight uptake data of Table 1).

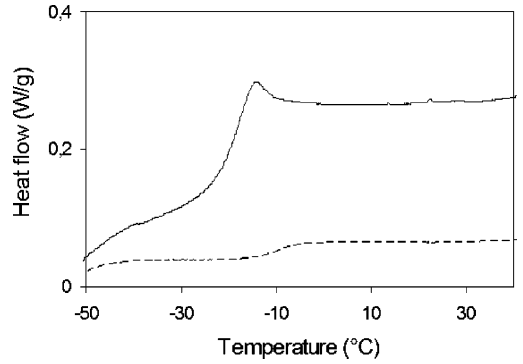

Figure 8. DSC scans showing the glass transition in *f*-PEA (solid line) and *g*-PEA (dashed line) from CotEA2. The thermograms are normalized with respect to the actual PEA weight fraction).

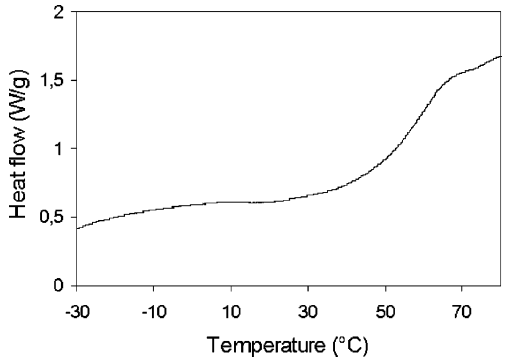

Figure 9. DSC heating scan showing the glass transition in the CotEA2Sty sample.

The modified fiber from sample CotEA2 presents a thermal transition at −10 °C associated with the glass transition temperature (T_g) of the *g*-PEA chains (Figure 8). This is higher than the T_g value reported for bulk PEA with a narrow M_w distribution and above the entanglement mass, M_e ($T_g \approx -19$ °C and $M_e \approx 12\,000$ g mol^{-1}, respectively[48]). However, the DSC analysis of the free polymer from CotEA2 (*f*-PEA of Figure 8) gave a T_g value of −19 °C, as expected from $\bar{M}_n \approx M_e = 11\,900$ g mol^{-1}. In agreement with the results of the ^{1}H FID analysis, the thermal behavior of *g*-PEA in the sample CotEA2 indicates a lower segmental mobility, with respect to that of bulk PEA, of the polymer anchored by one chain end to the fiber surface. It is worth mentioning that this is opposite to the response of thin films weakly interacting with the substrate, where the T_g decreases with decreasing thickness of the film.[49]

The above considerations are further confirmed by the measured Δc_p value of 4×10^{-3} J K^{-1} mol^{-1} for *g*-PEA in CotEA2, which compares to $\Delta c_p = 4 \times 10^{-2}$ J K^{-1} mol^{-1} for the *f*-PEA fraction from the same experiment, where the former is lower than the roughly 1.6×10^{-2} J K^{-1} mol^{-1} one would expect based on a simple scaling factor (the modified fibers from CotEA2 contain approximately 40 wt % *g*-PEA, according to the 67% measured weight uptake).

Only a broad second-order transition centered at $T = 46$ °C could be clearly detected in the first heating scan of CotEA2Sty (Figure 9). The results of the ^{1}H T_1 investigation indicate that mixing of the two homopolymer blocks is negligible on a 100 Å spatial scale, and thus the observed T_g must be associated with the *g*-PSty block. If one assumes that the average molecular weight of *g*-PSty must be comparable with that of *f*-PSty, then the T_g of the *g*-PSty block is quite lower than expected. Such behavior, opposite to that observed for *g*-PEA, could be explained as the result of effective decoupling of the *g*-PSty segmental motion from that of the rigid fiber surface promoted by the bridging, highly mobile *g*-PEA block. In other words, a phase-separated outer layer of PSty may behave as a thin film weakly interacting with the substrate, emphasizing the previously mentioned T_g-lowering effect deriving from a decreasing thickness of the film.

In Table 5 are also summarized the results from the thermogravimetric analyses. The onset of the pyrolytic weight loss ($T_{d,10}$) occurs at a slightly lower temperature in cotton-*g*-PEA than in pure cotton, possibly as a result of the presence of the less thermally stable brominated chain ends in the former. In the TGA curve of CotEA2 (Figure 10) the first of two main weight loss stages corresponds to the decomposition of cellulose, with a maximum rate at $T_{d,max} = 354$ °C; in the following stage the decomposition of *g*-PEA takes place with $T_{d,max} = 398$ °C, a temperature only slightly lower than that in *f*-PEA ($T_{d,max} = 403$ °C). The roughly 30% fractional weight loss in the second stage of the pyrolytic decomposition of CotEA2 compares fairly well with the 40 wt % of *g*-PEA determined from the weight uptake after the EA graft polymerization. The block copolymer structure improves the thermal stability of the modified fibers. Again, the initial weight loss due to the pyrolysis of cellulose (Figure 10), with $T_{d,10}$ comparable to that of pure cotton, is followed by a broad decomposition stage involving the whole block copolymer structure and $T_{d,max} = 403$ °C, the highest among the samples investigated increased stability of the graft copolymer.

Conclusion

The controlled growth of *g*-PEA from the surface of a BIBB-modified cotton fiber by the ATRP process and the effective reinitiation from the *g*-PEA-Br chain ends in the block copolymerization of Sty were achieved by the addition of either a sacrificial free initiator or Cu(II) as a deactivator to the system comprising monomer, fiber-grafted initiator, and Cu(I) catalyst. With the addition of Cu(II) the formation of free polymer is effectively reduced, although with some loss of control of the polymerization process as indicated by the broader PDI of the ungrafted fraction. Therefore, the synthesis in the presence of a sacrificial free initiator was preferred for the first stage (growth of *g*-PEA) to minimize the formation of dead chain ends that

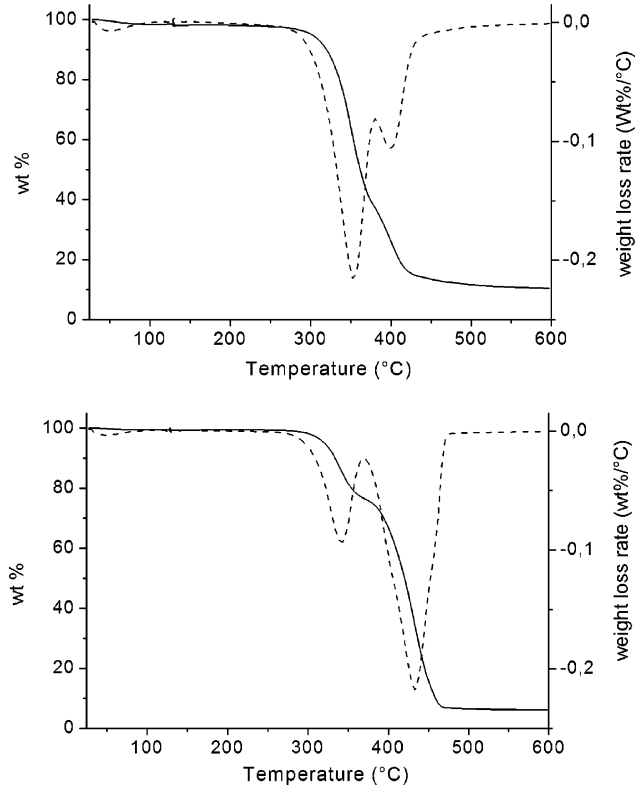

Figure 10. Pyrolytic weight loss curves (solid line) and weight loss rates (dashed line) from the TGA scans of CotEA2 (top) and CotEA2Sty (bottom).

would have been inactive in the reinitiation, thus preventing block copolymer growth.

Neither the *g*-PEA nor the *g*-PEA-*b*-PSty chains could be cleaved from the cellulose without degradation. However, separate grafting experiments with BMA, allowing us to successfully recover the PBMA grafts after selective hydrolysis of cotton-*g*-PBMA, confirmed the anticipated fair correspondence between $\bar{M}_n$ and PDI of the *f*-PBMA and *g*-PBMA fraction, respectively.

The efficiency of reinitiation by the halogen-terminated *g*-PEA chains in the block copolymerization with styrene could not be assessed directly. The PDI values of approximately 1.5 measured for the *f*-PSty fractions are still compatible with a controlled interfacial polymerization process. The EIC figures calculated from the SEC data indicate a reduction of approximately 1 order of magnitude of the surface density of active initiating species from the initial cellulose-OBIB to the polymer-grafted cellulose-*g*-PEA. However, such reduction is likely to result from a combination of irreversible terminations and kinetically inactive polymer-buried chain ends.

Both the thermal behavior and the molecular dynamics from the ^{1}H FID analysis indicate a lower segmental mobility of the PEA grafts anchored by one chain end to the fiber surface with respect to bulk PEA. This mobility further decreases when PEA-*b*-PSty chains are grafted to the cellulose fibers. It is worth mentioning that this is opposite to the response of thin films weakly interacting with the substrate, where the T_g decreases with decreasing thickness of the film.

Acknowledgment. The authors thank Professor C. A. Veracini for the helpful discussions, Mr. Piero Narducci for the SEM analyses, and the MIUR-NANOPACK FIRB 2003 program (Project No. D.D.2186 Prot.N.RBNE03R78E) for financial support.

Supporting Information Available. Determination of the M_w of cellulose-grafted PBMA and analytical functions adopted for the reproduction of the on-resonance FID curve. This material is available free of charge via the Internet at http://pubs.acs.org.

References and Notes

(1) Bikales, N. S.; Segal, L. In *Cellulose and Cellulose Derivatives*, 2nd ed.; Ott, E., Spurlin, H. M., Grafflin, M. W., Eds.; High Polymers 5; Wiley-Interscience: London, 1971.
(2) Atalla, R. H.; Gast, J. C.; Sindorf, D. W.; Bartuska, V. J.; Maciel, G. E. *J. Am. Chem. Soc.* **1980**, *102*, 3249−3251.
(3) Earl, W. L.; VanderHart, D. L. *Macromolecules* **1981**, *14*, 570−574.
(4) Gardner, K. H.; Blackwell, J. *Biopolymers* **1974**, *13*, 1975−2001.
(5) Sarko, A.; Muggli, R. *Macromolecules* **1974**, *7*, 486−494.
(6) Botaro, V. R.; Gandini, A.; Belgacem, M. N. *J. Thermoplast. Compos. Mater.* **2005**, *18*, 107−117.
(7) Mohanty, K.; Khan M. A.; Hinrichsen G. *Compos. Sci. Technol.* **2000**, *60*, 1115−1124.
(8) Flaqué, C.; Contat Rodrigo, L.; Ribes-Greus, L. *J. Appl. Polym. Sci.* **2000**, *76*, 326−335.
(9) Narayan, R.; Biermann, C. J.; Hunt, M. O.; Horn, D. P. In *Adhesives from Renewable Resources*; Conner, A. H., Branham, S. J., Eds; ACS Symposium Series 385; American Chemical Society: Washington, DC, 1989; Chapter 24, pp 337−354.
(10) Singh, B.; Gupta, M.; Verma, A.; Tyagi, O. S. *Polym. Int.* **2000**, *49*, 1444−1451.
(11) Joly, C.; Gauthier, R.; Chabert, B. *Compos. Sci. Technol.* **1996**, *56*, 761−765.
(12) Li, Y.; May, Y.-W.; Ye, L. *Compos. Sci. Technol.* **2000**, *60*, 2037−2055.
(13) Flaqué, C.; Montserrat, S. *J. Appl. Polym. Sci.* **1993**, *47*, 595−605.
(14) Okieimen, F. E.; Ogbeifun, D. E. *Eur. Polym. J.* **1996**, *32*, 311−315.
(15) Hafren, J.; Cordova, A. *Macromol. Rapid Commun.* **2005**, *26*, 82−86.
(16) Carlmark, A.; Malmström, E. E. *J. Am. Chem. Soc.* **2002**, *124*, 900−901.
(17) Carlmark, A.; Malmström, E. E. *Biomacromolecules* **2003**, *4*, 1740−1745.
(18) Lee, S. B.; Koepsel, R. R.; Morley, S. W.; Matyjaszewski, K.; Sun, Y.; Russell, A. J. *Biomacromolecules* **2004**, *5*, 877−882.
(19) Plackett, D.; Jankova, K.; Egsgaard, H.; Hvilsted, S. *Biomacromolecules* **2005**, *6*, 2474−2484.
(20) Huang, W.; Kim, J.-B.; Bruening, M. L.; Baker, G. *Macromolecules* **2002**, *35*, 1175−1179.
(21) Fischer, H. *Macromolecules* **1997**, *30*, 5666−5672.
(22) Matyjaszewski, K.; Miller, P. J.; Shukla, N.; Immaraporn, B.; Gelman, A.; Luokala, B. B.; Siclovan, T. M.; Kickelbick, G.; Vallant, T.; Hoffmann, H.; Pakula, T. *Macromolecules* **1999**, *32*, 8716−8724.
(23) Princi, E.; Vicini, S.; Pedemonte, E.; Gentile, G.; Cocca, M.; Martuscelli, E. *Eur. Polym. J.* **2006**, *42*, 51−60.
(24) Princi, E.; Vicini, S.; Proietti, N.; Capitani, D. *Eur. Polym. J.* **2005**, *41*, 1196−1203.
(25) Margutti, S.; Vicini, S.; Proietti, N.; Capitani, D.; Conio, G.; Pedemonte, E.; Segre, A. L. *Polymer* **2002**, *43*, 6183−6194.
(26) Mais, U.; Binder, W. H.; Knaus, S.; Gruber, H. *Macromol. Chem. Phys.* **2000**, *201*, 2115−2122.
(27) Ge, S.; Guo, L.; Rafailovich, M. H.; Sokolov, J.; Overney, R. M.; Buenviaje, C.; Peiffer, D. G.; Schwarz, S. A. *Langmuir* **2001**, *17*, 1687−1692.
(28) Keller, R. N.; Wycoff, H. D. *Inorg. Synth.* **1946**, *2*, 1.
(29) Kitamaru, R.; Horii, F.; Murayama, K. *Macromolecules* **1986**, *19*, 636−643.
(30) Stana-Kleinschek, K.; Ribitsch, V. *Colloids Surf., A* **1998**, *140*, 127−138.
(31) Hon, D. N.-S.; Yan, H. *J. Appl. Polym. Sci.* **2001**, *81*, 2649−2655.
(32) Fernandez Garcia, M.; De la Fuente, J. L.; Cerrada, M. L.; Madruga, E. L. *Polymer* **2002**, *43*, 3173−3179.
(33) Thiebaud, S.; Borredon, M. E. *Bioresour. Technol.* **1998**, *63*, 139−145.
(34) Prucker, O.; Rühe, J. *Macromolecules* **1998**, *31*, 592−601.
(35) Ejaz, M.; Tsuji, Y.; Fukuda, T. *Polymer* **2001**, *42*, 6811−6815.
(36) Bontempo, D.; Tirelli, N.; Feldman, K.; Masci, G.; Crescenzi, V.; Hubbell, J. A. *Adv. Mater.* **2002**, *14*, 1239−1241.

(37) Luzinov, I.; Voronov, A.; Minko, S.; Kraus, R.; Wilke, W.; Zhuk A. *J. Appl. Polym. Sci.* **1996**, *61*, 1101−1109.
(38) Masuda, K.; Adachi, M.; Hirai, A.; Yamamoto, H.; Kaji, H.; Horii, F. *Solid State Nucl. Magn. Reson.* **2003**, *23*, 198−212.
(39) Calucci, L.; Galleschi, L.; Geppi, M.; Mollica, G. *Biomacromolecules* **2004**, *5*, 1536−1544.
(40) Di Colo, G.; Baggiani, A.; Zambito, Y.; Mollica, G.; Geppi, M.; Serafini, M. F. *Int. J. Pharm.* **2006**, *310*, 154−161.
(41) Borsacchi, S.; Cappellozza, S.; Catalano, D.; Geppi, M.; Ierardi, V. *Biomacromolecules* **2006**, *7*, 1266−1273.
(42) Ferrini, V.; Forte, C.; Geppi, M.; Pizzanelli, S.; Veracini, C. A. *Solid State Nucl. Magn. Reson.* **2005**, *27*, 215−222.
(43) Kristiansen, P. E.; Hansen, E. W.; Pedersen, B. *J. Phys. Chem. B* **1999**, *103*, 3552−3558.
(44) Mackay, A. L.; Tepfer, M.; Taylor, I. E. P.; Volke, F. *Macromolecules* **1985**, *18*, 1124−1129.
(45) McBrierty, V. J.; Packer, K. J. *Nuclear Magnetic Resonance in Solid Polymers*; Cambridge University Press: Cambridge, U. K., 1993.
(46) Bardet, M.; Emsley, L.; Vincendon, M. *Solid State Nucl. Magn. Reson.* **1997**, *8*, 25−32.
(47) Geppi, M.; Harris, R. K.; Kenwright, A. M.; Say, B. J. *Solid State Nucl. Magn. Reson.* **1998**, *12*, 15−20.
(48) Andreozzi, L.; Castelvetro, V.; Faetti, M.; Giordano, M.; Zulli, F. *Macromolecules* **2006**, *39*, 1880−1889.
(49) Ao, Z. M.; Jiang, Q. *Langmuir* **2006**, *22*, 1241−1246.

BM060602W